Science of the Total Environment 573 (2016) 55–65

Contents lists available at ScienceDirect

Science of the Total Environment

journal homepage: www.elsevier.com/locate/scitotenv

Identification and influence of spatio-temporal outliers in urban air quality measurements☆

Brendan O'Leary [a], John J. Reiners Jr. [a], Xiaohong Xu [b], Lawrence D. Lemke [a,]*

[a] Wayne State University, Detroit, MI, USA
[b] University of Windsor, Windsor, Ontario, Canada

HIGHLIGHTS

- Four alternative outlier identification methods were evaluated.
- Local and global methods were used in combination to identify outliers.
- Using multiple methods increases confidence in outlier identification.
- Outlier removal weakened associations between air pollution and asthma.
- Incorporation of temporal trends improved air pollution-asthma associations.

GRAPHICAL ABSTRACT

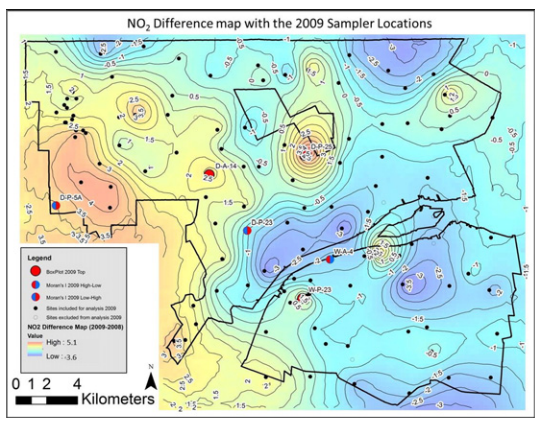

ARTICLE INFO

Article history:
Received 9 May 2016
Received in revised form 4 August 2016
Accepted 5 August 2016
Available online 20 August 2016

Editor: D. Barcelo

Keywords:
Outlier
Spatio-temporal

ABSTRACT

Forty eight potential outliers in air pollution measurements taken simultaneously in Detroit, Michigan, USA and Windsor, Ontario, Canada in 2008 and 2009 were identified using four independent methods: box plots, variogram clouds, difference maps, and the Local Moran's I statistic. These methods were subsequently used in combination to reduce and select a final set of 13 outliers for nitrogen dioxide (NO_2), volatile organic compounds (VOCs), total benzene, toluene, ethyl benzene, and xylene (BTEX), and particulate matter in two size fractions ($PM_{2.5}$ and PM_{10}). The selected outliers were excluded from the measurement datasets and used to revise air pollution models. In addition, a set of temporally-scaled air pollution models was generated using time series measurements from community air quality monitors, with and without the selected outliers. The influence of outlier exclusion on associations with asthma exacerbation rates aggregated at a postal zone scale in both cities was evaluated.

Abbreviations: BTEX, total benzene, toluene, ethyl benzene, and xylene; GeoDHOC, Geospatial Determinants of Health Outcomes Consortium; ICD-9-CM, international classification of diseases, ninth revision, clinical modification; ICD-10, international classification of diseases, tenth revision;; IQR, interquartile range; MASN, Michigan air sampling network; MDEQ, Michigan Department of Environmental Quality; NO_2, nitrogen dioxide; PAHs, polycyclic aromatic hydrocarbons; PM, particulate matter; QA/QC, quality assurance/quality control; SO_2, sulfur dioxide; VOCs, volatile organic compounds.

☆ Funding sources and IRB approval: Support for this project was provided by a grant from the W.K. Kellogg Foundation, P3018205, and through a Wayne State University Career Development Grant. Institutional Review Board approval for the original asthma study (reported in Lemke et al., 2014) was obtained from the participating institutions (IRB# 073508B3X) and all personal and health information was de-identified and coded to protect the identity of individuals. IRB approval for a subsequent study, which funded the outlier evaluation and temporal scaling of air pollution reported in this paper, was obtained through Wayne State University (IRB# 091012MP2E).

* Corresponding author at: Department of Geology, Room 0224 Old Main, 4841 Cass, Detroit, MI 48202, USA.
E-mail address: LDLemke@wayne.edu (L.D. Lemke).

http://dx.doi.org/10.1016/j.scitotenv.2016.08.031

Intraurban variation
Air pollution
Asthma

Results demonstrate that the inclusion or exclusion of outliers influences the strength of observed associations between intraurban air quality and asthma exacerbation in both cities. The box plot, variogram cloud, and difference map methods largely determined the final list of outliers, due to the high degree of conformity among their results. The Moran's I approach was not useful for outlier identification in the datasets studied. Removing outliers changed the spatial distribution of modeled concentration values and derivative exposure estimates averaged over postal zones. Overall, associations between air pollution and acute asthma exacerbation rates were weaker with outliers removed, but improved with the addition of temporal information. Decreases in statistically significant associations between air pollution and asthma resulted, in part, from smaller pollutant concentration ranges used for linear regression. Nevertheless, the practice of identifying outliers through congruence among multiple methods strengthens confidence in the analysis of outlier presence and influence in environmental datasets.

1. Introduction

Environmental data often include anomalous measurements that require researchers to decide whether to include or exclude them from study datasets and subsequent analyses. Experimental integrity may dictate that all measurements passing QA/QC protocols be included, even at the risk of including erroneous measurements that could lead to inaccurate interpretations. Conversely, exclusion of unusual measurements could mask important phenomena reflected by anomalous, yet accurate, measurements. This problem is particularly acute for environmental studies involving space-time series datasets with large numbers of measurements that increase the potential for outliers.

In response, a number of approaches have been employed to identify outliers in spatio-temporal datasets (Dai et al., 2016; Schubert et al., 2014). In the most generic sense, a statistical outlier deviates markedly from other members of a sample group (Barnett and Lewis, 1994). Clougherty et al. (2013), for instance, defined outliers as air quality measurements falling more than ± 3 standard deviations away from the mean. Others have employed the Moran's I statistic to identify spatial outliers in geomorphic changes to sand dunes after vegetation removal (Walker et al., 2013), and to detect and eliminate spatial outliers in urban soil lead measurements (Zhang et al., 2008) and agricultural soil phosphorus measurements (Fu et al., 2016). In air pollution studies, Kracht et al. (2013) utilized a low pass filter to identify and remove high concentrations while preserving low frequencies in European air pollutant time series measurements. Zou et al. (2014) employed a spatial autocorrelation based cluster analysis to detect disproportionate patterns of air pollution exposure across the continental United States. These, and other studies (Anastasopoulos et al., 2012; Li et al., 2014; Sguera et al., 2016; Szpiro et al., 2009; Wu et al., 2010), illustrate the need to specify criteria for the definition of outliers in environmental datasets.

Spatio-temporal datasets inherently contain two types of information: attribute and location. Attribute information comprises a set of measurements associated with each point in time or space. Location information provides the associated spatial and/or temporal context of each attribute measurement. Attribute and location information can be assessed separately and jointly to identify potential outliers. Consequently, an outlier can be considered *global* when its value deviates from the entire dataset or *local* if its value deviates from the points immediately surrounding it in time or space (Ernst and Haesbroeck, 2016).

This study evaluated alternative methods of outlier identification in a set of air quality measurements collected by the Geospatial Determinants of Health Outcomes Consortium (GeoDHOC) in Detroit, Michigan, USA and Windsor, Ontario, Canada in 2008 and 2009 (Miller et al., 2010). The objective was to determine if outliers were present in the datasets and, if so, to evaluate their impact on modeled pollution distributions, and pollution-asthma associations. Multiple outlier identification techniques including boxplots, variogram clouds, difference maps, and the Local Moran's I statistic were applied individually and in combination. This study leverages prior investigations that associated acute asthma exacerbations with exposure estimates derived from the GeoDHOC air pollutant models in Detroit and Windsor (Lemke et al., 2014). The influence of temporal interpolation (O'Leary and Lemke, 2014) and outlier removal were analyzed by revising prior air pollution models to exclude outliers and reevaluating subsequent associations with asthma exacerbations in Detroit and Windsor.

2. Methods

2.1. Project datasets

The air pollution and asthma datasets utilized in this study are described in detail by Miller et al. (2010); O'Leary and Lemke (2014), and Lemke et al. (2014). Briefly, the GeoDHOC measured simultaneous concentrations of nitrogen dioxide (NO_2), sulfur dioxide (SO_2), volatile organic compounds (VOCs), polycyclic aromatic hydrocarbons (PAHs), and particulate matter (PM) in three size fractions (PM_1, $PM_{1-2.5}$, and $PM_{2.5-10}$) during two, two-week air sampling periods between September 5–20, 2008 and May 29–June 13, 2009 (Miller et al., 2010). A total of 50 active samplers measuring PM and PAHs and 100 passive samplers measuring NO_2, SO_2, and VOCs were deployed in 2008 (Fig. 1). All sites with active samplers also included collocated passive samplers. In 2009, a nearly identical sampling plan was implemented that included 50 active samplers and 133 passive samplers. Thirty three additional passive samplers were added in new locations in 2009 to create a transect across a primary road in Windsor and evaluate shorter-scale variation in one neighborhood in Detroit (Fig. 1). Measurements made with passive and active samplers had an approximate spatial density of 5 km^2 per sample and 10 km^2 per sample, respectively, throughout both cities. These measurements were interpolated using ordinary kriging to generate air pollution estimates across Detroit and Windsor on a 300 by 300 meter grid (Miller et al., 2010).

O'Leary and Lemke (2014) merged the spatially detailed GeoDHOC dataset with time series measurements of NO_2, benzene, toluene, ethylbenzene, and xylene (BTEX), and PM recorded at five Michigan Air Sampling Network (MASN) stations (MDEQ, 2008, 2013) in the city of Detroit (Fig. 1). The result was a monthly series of temporally interpolated air pollution models for NO_2, BTEX, $PM_{2.5}$, and PM_{10} spanning a three year period from 2008 to 2010.

Lemke et al. (2014) used diagnostic coding from clinical encounters to assess asthma prevalence rates and acute asthma exacerbation for individuals 5–89 years of age living in Detroit and Windsor. Acute asthma events included both hospital admissions and emergency department visits with primary diagnoses of asthma identified using the appropriate ICD9-CM codes (493.xx) or ICD-10 code (J45). In Detroit, geocoding by residential address was used to assign a spatial location to health outcome event records and asthma counts within 25 zip code tabulation areas. Windsor records were assigned to one of twelve 3-digit postal forward sortation areas based on residential address. Within each postal code area, asthma counts were stratified by age and gender to account for differences in the age-gender distribution of the underlying study population. Institutional Review Board approval for the study was

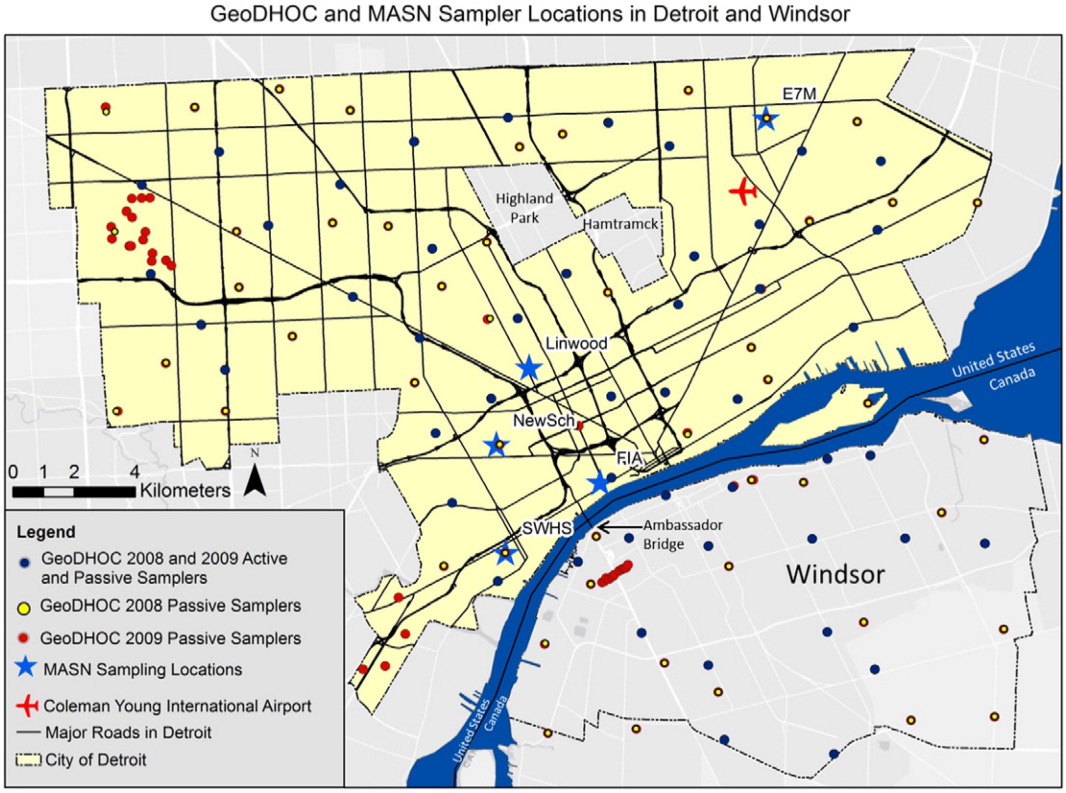

Fig. 1. Map of Detroit and Windsor GeoDHOC 2008 and 2009 sampling locations and Michigan Air Sampling Network (MASN) sampling locations.

obtained from the participating institutions and all personal and health information was de-identified and coded to protect the identity of individuals.

2.2. Outlier detection

Potential outliers in the 2008 and 2009 GeoDHOC air pollution measurement dataset were identified using four independent methods. Identification methods (Fig. 2) included both quantitative (box plots and Local Moran's I) and qualitative (variogram clouds and difference maps) approaches that were implemented using SpaceStat 3.0 (Biomedware Inc.) and Surfer 12 (Golden Software) commercial software packages. Air pollutant analytes examined included NO_2, BTEX, total VOCs, $PM_{2.5}$, PM_{10}, and PAHs.

A two-step process was implemented to narrow the field of potential outliers identified using each of the four methods independently. First, potential outliers were compared and those identified by only a single method were disregarded. Second, each remaining potential outlier was assessed using combinations of the four methods (Fig. 2) to determine a final set of outliers for subsequent analysis in this study.

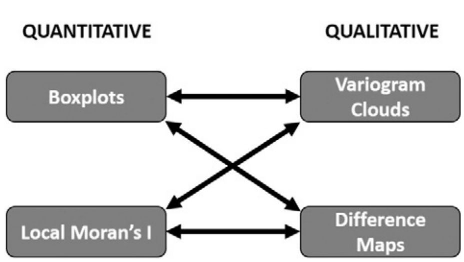

Fig. 2. Methods used individually and in combination to evaluate outliers.

2.2.1. Identification of potential outliers

Box plots, which provide aspatial representations of the spread of concentration distributions, were used to identify anomalous values among the global population of measurements for each pollutant. In each plot, the box represented the interquartile range and whiskers delineated the region occupied by ± 1.5 times the interquartile range beyond the box boundaries. For this study, points plotting above or below the whiskers were identified as potential outliers. Histograms were also examined to confirm that these points were located at distribution extremes for each dataset.

Variogram clouds (Haslett et al., 1991), in which the dissimilarity (square root of the absolute difference) between two measurement locations is plotted as a function of their Euclidean distance, were used to assess dataset spatial variability. Measurement points located close together are expected to display more similarity than points separated by a greater geographical distance (Isaaks and Srivastava, 1989). Consequently, pairs of points displaying high dissimilarity over a geographically small distance were initially considered potential outliers for this study. This approach was found to be too general, however, and was subsequently refined to exclude variogram cloud pairs that did not also include points corresponding to box plot anomalies.

Two approaches were used to identify potential outliers based on differences between September 2008 and June 2009 GeoDHOC measurements. In the first instance, points with measurements from both sampling events were compared to identify large positive or negative changes between the two sampling periods. These were considered potential outliers for both the 2008 and 2009 events. Although most samplers were deployed in the same locations in 2008 and 2009, QA/QC protocols (Miller et al., 2010) led to the exclusion of measurements from different locations in each sampling period. Therefore, a second approach was employed to incorporate information from sample points with only one measurement (including additional locations added during 2009 sampling).

Grid arithmetic was used to generate difference maps by subtracting the September 2008 from the June 2009 ordinary kriged model grids for each analyte. Positive regions on each difference map represent areas where measured and interpolated concentrations increased between sampling events. Earlier potential anomalies identified on the basis of large changes between 2008 and 2009 were evident on difference maps as 'bullseye' shaped isoconcentration lines centered on single sampler locations. Other, more subtle features associated with measurements available in only one year that contrasted with modeled values interpolated from nearby measurement points in the other year, were also considered potential anomalies. In addition, some difference maps included anomalously high or low values adjacent to, but offset from, individual sampling locations. These features can originate as artifacts from gridding or contouring algorithms when closely spaced control points have markedly different values. The resulting 'bullseye' constitutes a potentially inaccurate model estimate and thus the measured value at the adjacent sampling location was therefore considered a potential outlier.

The Local Moran's I function (Anselin, 1995) assumes a normal population to evaluate spatial distributions with spatial randomness representing the null hypothesis. The Jarque-Bera test was used to test for normality (Kiefer and Salmon, 1983) by examining the GeoDHOC dataset for each analyte in September 2008 and June 2009. If the dataset generated a p-value ≤ 0.05, it was determined to be non-normal and, consequently, a normal score transform was performed. Subsequently, the Moran's I was calculated using the following equation:

$$I_i = z_i \sum_{j=1}^{n} w_{i,j} z_j,\ i \neq 1$$

where I is the Moran's I coefficient, z is the z score, w is a weighting parameter applied to the neighbors, i identifies the sample point being evaluated, j is an index value corresponding to each of the nearby neighbors, and n is the number of neighbors (Anselin, 1995). A value of zero indicates no spatial autocorrelation. Positive I_i values indicate that there is either a cluster of low or high values. Negative I_i values indicate that high and low values are clustered together.

This study used 999 Monte Carlo simulations in SpaceStat to derive a p-value for each sampler location. The point adjacency method was set to the nearest 8 neighbors and the neighbor weight method was standardized to neighbor count, ensuring that I_i only reflected the immediate surrounding sampler locations and rendering the Local Moran's I an appropriate tool for local outlier identification. Consequently, potential outliers were identified as sampling points with a negative I_i value along with a p-value ≤ 0.05. These represent either sampling points with higher values than the surrounding sampling locations (high-low) or lower values that the surrounding sampling locations (low-high).

2.2.2. Outlier selection

Potential outliers initially determined using each of the independent methods described above were compared, and outliers identified by only one of the four methods were discarded. Combinations of the methods (Fig. 2) were subsequently used to evaluate and select outliers from the remaining potential outliers. This approach combined quantitative and qualitative measures and provided a means of selecting outliers for further analysis with greater confidence.

Variogram clouds were used in conjunction with box plots to evaluate pairs of points associated with extreme values. Potential box plot outliers were highlighted within variogram cloud plots to identify sampling points yielding pairs that fell within the region of high variability versus minimal separation distance. This approach represents a hybrid identification method that combines information from both global (box plot) and local (variogram cloud) outlier indicators.

Measurements identified as potential outliers using the Local Moran's I statistic were also evaluated in conjunction with variogram clouds to assess agreement for local outlier identification. Again, measurement points identified as potential outliers using the Local Moran's I were highlighted within variogram cloud plots to assess whether they contributed to pairs falling within the region of high variability versus minimal separation distance.

In separate analyses, locations of outlier measurements identified with box plot analysis and Local Moran's I were annotated on the associated difference maps using identifying symbols to facilitate comparisons among these methods. This approach highlighted relationships between box plot and Moran's I outlier locations and areas of steep concentration gradients present on the difference maps. Unlike the comparatively straightforward process of recognizing outliers in regularly-spaced time-series measurements, temporal differences in this study were based on two widely-spaced sampling events. Difference map anomalies arising from measurement contrasts could therefore result from outliers in either the 2008 or 2009 dataset. In addition to examining the original 2008 and 2009 air pollution maps, evaluating the correspondence between difference map anomalies and outliers identified using alternative methods (i.e. boxplots and Moran's I) provided a useful means to determine which sampling event gave rise to the potential outliers identified on each difference map.

The final selection of outliers entailed the development of a decision rule that required the correspondence of outlier identification on two or more of the boxplot, variogram cloud, and Moran's I statistic, coupled with recognizable anomalies on difference maps for concentrations measured between 2008 and 2009.

2.3. Air pollution model revision

Selected outliers were removed from the 2008 and 2009 GeoDHOC datasets and revised models were generated for affected air pollutants using ordinary kriging and temporal interpolation following procedures outlined in Miller et al. (2010) and O'Leary and Lemke (2014), respectively. In formulating new variogram models and kriging parameters, an attempt was made to adhere to the parameters of the original models as closely as possible; however, changes to several parameters were necessary. The most important modifications involved reduced variogram ranges and sill contributions resulting from decreased variance observed when extreme outlier values were excluded. To facilitate comparison of asthma associations, particulate matter models originally mapped by Miller et al. (2010) in PM_1, $PM_{1-2.5}$, and $PM_{2.5-10}$ size fractions were summed to the cumulative $PM_{2.5}$ and PM_{10} size fractions regulated in the US and Canada and used by Lemke et al. (2014). These changes are described in detail by O'Leary (2014).

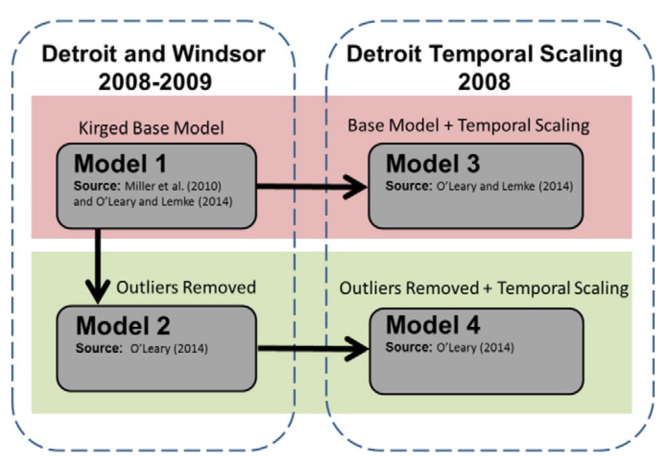

Fig. 3. Summary of the four models used in this study.

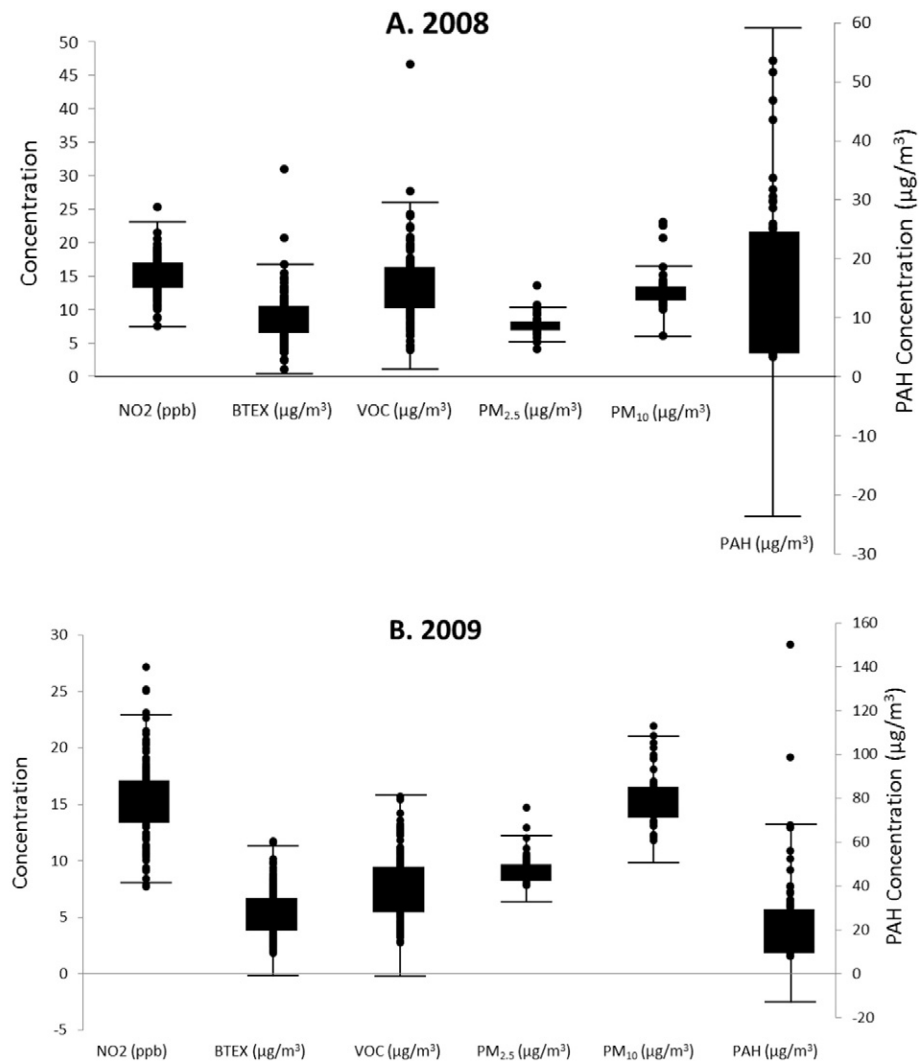

Fig. 4. Box plots for each analyte in A) 2008 and B) 2009. Potential outliers fall above or below the whisker lines. See Supplemental Table 1 for relevant plot values. Note the vertical access on the left corresponds to NO_2, BTEX, Total VOC, $PM_{2.5}$, and PM_{10}. The axis on the right side of the graph corresponds to PAH.

Air pollution model revisions generated four sets of alternative models (Fig. 3). Model 1 constitutes the original September 2008 and June 2009 GeoDHOC ordinary kriged models for the Detroit-Windsor Airshed. Outliers were removed from Model 1 to create Model 2. Model 3 was derived from the incorporation of Detroit MASN data by O'Leary and Lemke (2014). It includes temporal scaling of NO_2, BTEX, $PM_{2.5}$ and PM_{10} for 12 months in 2008 and is applicable only to Detroit. Model 4 was generated from Model 2 with outliers removed. It also incorporated temporal scaling for 12 months in 2008, and applies only to Detroit.

2.4. Asthma associations

Associations between acute asthma events and each revised air pollution model were assessed using the SpaceStat aspatial linear regression tool and compared to the Model 1 asthma associations reported by Lemke et al. (2014). Because asthma data were aggregated at the zip code scale in Detroit and the equivalent forward sortation area scale in Windsor ((Lemke et al., 2014), air pollutant model concentrations were averaged over each of the postal regions for this study.

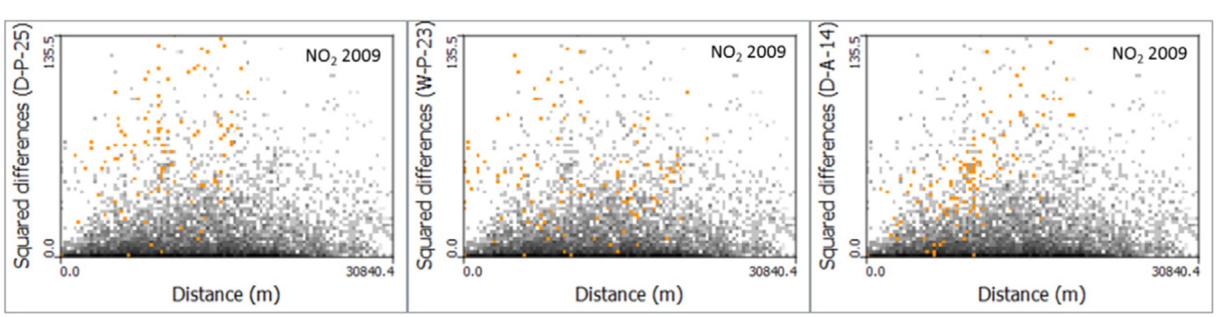

Fig. 5. Example variogram clouds for NO_2 2009. Highlighted points in each plot are associated with a single potential outlier identified through the boxplot method. D-P-25 and W-P-23 were classified as potential outliers based on the variogram plots shown.

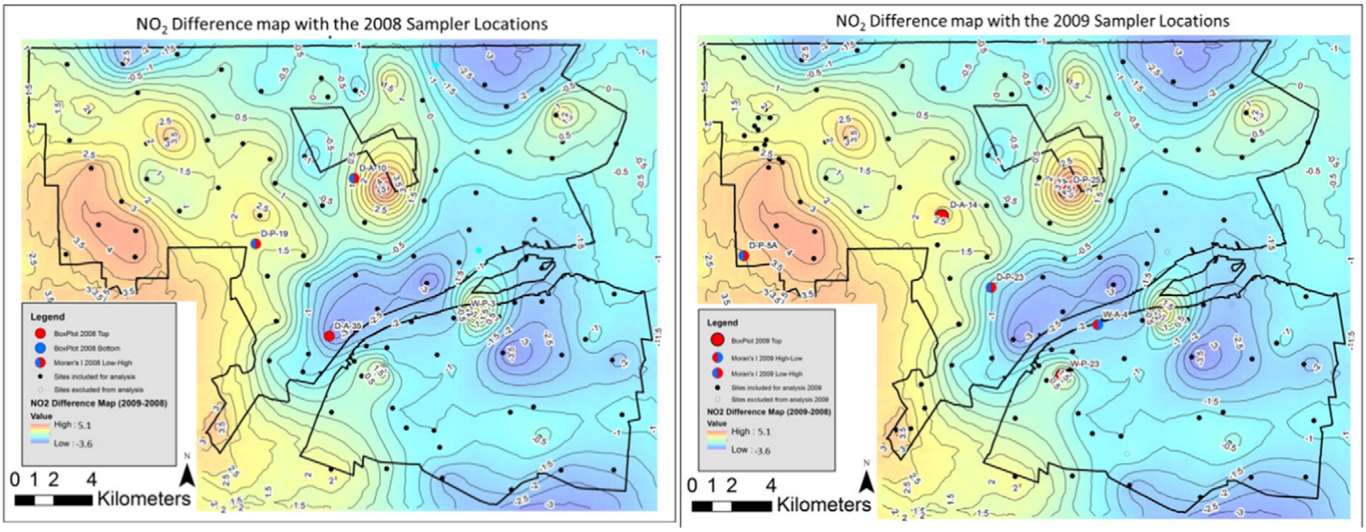

Fig. 6. Annotated NO_2 difference maps from 2008 and 2009.

Lemke et al. (2014) also relied upon cumulative asthma data for 2008. Therefore, twelve individual months were averaged to create a corresponding annual 2008 concentration for Model 3 and Model 4 in each Detroit zip code tabulation area.

3. Results and discussion

The results of potential outlier identification, final outlier selection, air pollution model revision, and asthma association reassessment are described and discussed below. Individual sample sites are designated by codes beginning with the letters 'D' or 'W' for locations in Detroit or Windsor. Sites with a combination of active and passive samplers include the letter 'A' and sites with only passive samplers include the letter 'P' followed by the station number (e.g., D-A-21 for active/passive sampler station 21 in Detroit; or W-P-4 for passive only sampler station 4 in Windsor).

3.1. Potential outlier identification

No single method, among the four used, emerged to definitively determine outliers for each analyte. Box plots (Fig. 4) revealed 24 potential outliers that exceeded the interquartile range $\pm$ 1.5 times the interquartile range (Supplemental Table 1). Values at or above the upper whisker were observed at 21 sampling locations and values at or below the lower whisker were found at 3 locations.

Similarly, the variogram cloud analysis coupled with box plot results (Fig. 5, Supplemental Fig. 1) identified thirteen sampling locations with a high degree of dissimilarity over a short geographical distance that were identified as potential outliers. All but one of these points were sampling locations with concentrations plotting above the top whisker in the corresponding box plot.

Sixteen potential outliers were identified using difference maps, including sampling points with large concentration contrasts between the September 2008 and June 2009 sampling periods, as well as a number of subtler features (Fig. 6, Supplemental Fig. 2). Twelve of these corresponded to potential outliers indicated by box plots, but only one was associated with samples identified as potential outliers using the Local Moran's I statistic.

The Local Moran's I test generated 22 statistically significant points (p-value ≤ 0.05) that showed spatial patterns of outliers (Table 1). Of these, 18 were classified as low-high, meaning the sampling points had a lower concentration than the surrounding points. The remaining four points were classified as high-low points, indicating the sampling points had a higher concentration than the surrounding samplers. 19 of the 22 potential outliers identified with the Moran's I were measured with passive air samplers.

Results from the Local Moran's I did not agree well with the other data outlier identification methods. With the exception of W-A-4 for $PM_{2.5}$ in 2008, potential Moran's I outliers were not identifiable as potential outliers on variogram clouds (Fig. 7). This was surprising because, in theory, both the Local Moran's I and variogram clouds can be used to identify local spatial outliers. With the exception of W-A-4 $PM_{2.5}$ in 2008, concentration measurements at points identified using Moran's I results fell within the boxplot interquartile range indicating that they were not global outliers. Likewise, with the same exception, the location of potential Moran's I outliers did not correspond to locations of potential outliers on the difference maps (Fig. 6, Supplemental Fig. 2).

Two potential explanations for the lack of Moran's I agreement with the other methods are its limited sample space as well as the nature of the air pollution datasets used in this study. Unlike the other methods, Moran's I statistic calculations were restricted to the nearest 8 neighbors of each point. This was expected to be a strength of the Moran's I approach because it is designed to identify local anomalies. However, the

Table 1
Statistically significant Local Moran's I results.

Analyte	Year	Site ID	Concentration	Units	Moran's I value	High/low	p-Value
NO_2	2008	D-A-10	15.1	ppb	−0.20	Low-high	0.002
NO_2	2008	D-P-19	15.0	ppb	−0.21	Low-high	<0.001
NO_2	2009	W-A-4	15.5	ppb	−0.10	High-low	0.048
NO_2	2009	D-P-23	15.1	ppb	−0.07	Low-high	0.016
NO_2	2009	D-P-5A	14.5	ppb	−0.28	Low-high	0.026
BTEX	2008	W-P-7	9.6	μg/m³	−0.23	High-low	0.022
BTEX	2008	D-A-34	8.6	μg/m³	−0.16	Low-high	0.024
BTEX	2008	D-P-2	7.6	μg/m³	−0.37	Low-high	0.008
BTEX	2009	W-P-2	5.6	μg/m³	−0.03	High-low	0.024
BTEX	2009	D-P-27	5.1	μg/m³	−0.15	Low-high	0.04
BTEX	2009	D-A-8	5.0	μg/m³	−0.19	Low-high	0.022
BTEX	2009	D-A-10	5.0	μg/m³	−0.26	Low-high	0.006
BTEX	2009	D-P-12	4.6	μg/m³	−0.31	Low-high	0.018
VOC	2008	D-A-34	13.5	μg/m³	−0.13	Low-high	0.004
VOC	2008	D-P-2	12.0	μg/m³	−0.38	Low-high	0.012
VOC	2008	D-P-25	12.9	μg/m³	−0.17	Low-high	0.034
VOC	2009	D-A-10	6.9	μg/m³	−0.19	Low-high	0.002
VOC	2009	D-P-12	6.7	μg/m³	−0.21	Low-high	0.012
VOC	2009	D-P-27	6.6	μg/m³	−0.25	Low-high	0.018
$PM_{2.5}$	2008	W-A-4	13.4	μg/m³	−1.44	High-low	0.046
PAH	2008	D-A-15	18.3	μg/m³	−0.03	Low-high	<0.001
PAH	2009	D-A-24	16.8	μg/m³	−0.61	Low-high	0.014

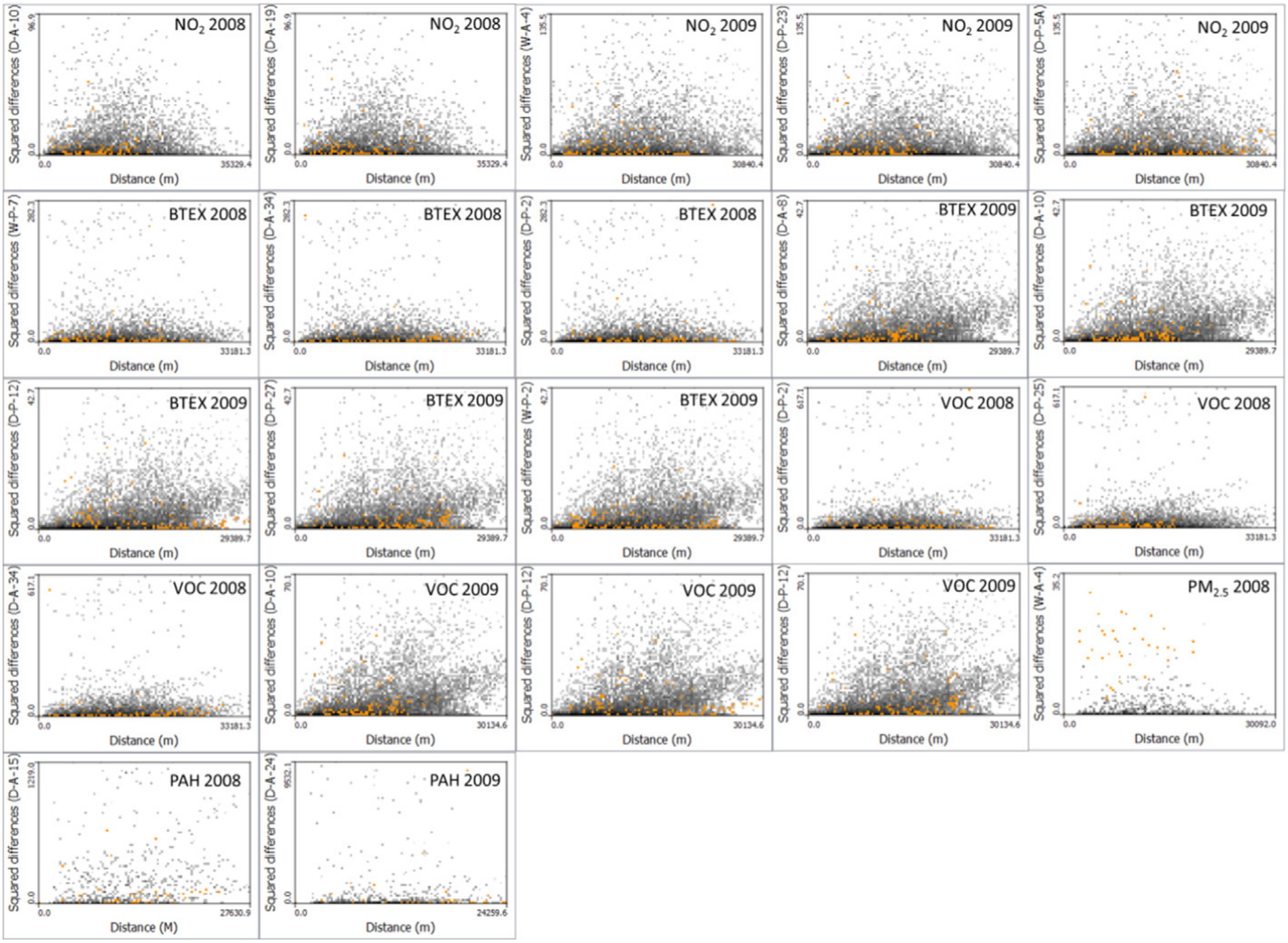

Fig. 7. Variogram clouds highlighting potential outliers identified using Moran's I results. W-A-4 $PM_{2.5}$ 2008 was identified as a potential outlier.

number of samplers in this study, which varied from 37 for pollutants measured with active samplers to 98 for passive samplers in the September 2008 dataset, may limit Moran's I effectiveness as a local outlier determinant because fewer samplers results in increased physical distance between samplers. Although the number of spatially distributed samplers employed in this study is large compared to most urban air quality studies, other environmental applications of the Local Moran's I used larger datasets (Li et al., 2013; Zhang et al., 2008; Zhang and McGrath, 2004; Zou et al., 2014).

Because of the poor association of the local Moran's I results with the other methods used in this study, the 21 unique points identified using the Moran's I statistic were dropped from the list of potential outliers. This left one sample, W-A-4 $PM_{2.5}$ in 2008, with overlap between the Moran's I and one or more of the other methods.

After omitting the 21 unique Moran's I potential outliers, 27 potential outliers remained (Table 2). Ten of these locations were identified by only one of the three remaining outlier detection methods, and were subsequently dropped as potential outliers. This resulted in a 'short list' of 17 potential outliers to be evaluated.

3.2. Outlier selection

The final selection of outliers was based on congruence among the identification methods employed, but nevertheless required judgement because different combinations of concurrence among methods were present (Table 2). The nine samples identified as potential outliers using three or more of the methods were selected as outliers. Four

Table 2
Summary table of potential spatial data outliers identified in the GeoDHOC 2008 and 2009 datasets. Check marks indicate sampling locations identified as potential outliers by that method. Shading indicates sample locations ultimately determined to be an outlier. IQR is interquartile range and mes. diff. is measured difference (June 2009–Sept. 2008).

Year	Analyte	Units	Site ID	Value	± 1.5 IQR	Box plot location	Box plot	Variogram cloud	Difference map	Mes. diff.
2008	NO_2	ppb	D-A-35	25.2	22.7	Top	✓	✓	✓	-4.5
2008	NO_2	ppb	W-P-3	7.3	7.5	Bottom	✓	✓	✓	7.9
2009	NO_2	ppb	D-P-25	27.1	23.5	Top	✓	✓	✓	-7.9
2009	NO_2	ppb	D-A-14	25.2	23.5	Top	–	–	–	3.8
2009	NO_2	ppb	W-P-23	25.0	23.5	Top	✓	✓	–	-
2008	BTEX	μg/m³	D-A-25	30.9	16.8	Top	✓	✓	✓	-19.3
2008	BTEX	μg/m³	D-A-5	20.5	16.8	Top	✓	–	–	-8.8
2009	BTEX	μg/m³	D-A-25	11.6	11.3	Top	✓	–	–	-19.3
2009	BTEX	μg/m³	D-A-5	11.7	11.3	Top	✓	✓	–	-8.8
2009	BTEX	μg/m³	D-A-33	9.8	11.3	-	–	–	✓	8.8
2008	VOC	μg/m³	D-A-25	46.6	26.4	Top	✓	✓	✓	-30.9
2008	VOC	μg/m³	D-A-5	27.6	26.4	Top	✓	–	–	-12.1
2009	VOC	μg/m³	D-A-25	15.7	15.4	Top	✓	–	–	-30.9
2009	VOC	μg/m³	D-A-33	13.0	15.4	-	–	–	✓	8.7
2008	$PM_{2.5}$	μg/m³	W-A-2	3.9	5.0	Bottom	✓	–	✓	5.7
2008	$PM_{2.5}$	μg/m³	D-A-6	10.5	10.1	Top	✓	–	–	-0.2
2008	$PM_{2.5}$	μg/m³	W-A-4	13.4	10.1	Top	✓	✓	✓	-5.5
2009	$PM_{2.5}$	μg/m³	W-A-8	14.7	12.2	Top	✓	✓	✓	7.3
2009	$PM_{2.5}$	μg/m³	D-A-33	12.9	12.2	Top	✓	–	✓	3.8
2008	PM_{10}	μg/m³	W-A-2	5.9	7.4	Bottom	✓	–	✓	9.9
2008	PM_{10}	μg/m³	D-A-32	23.0	17.1	Top	✓	✓	–	-1.9
2008	PM_{10}	μg/m³	D-A-6	22.5	17.1	Top	✓	✓	–	-3.1
2008	PM_{10}	μg/m³	W-A-4	2.6	17.1	Top	✓	–	–	-8.3
2009	PM_{10}	μg/m³	W-A-8	21.9	21.1	Top	✓	✓	✓	10.3
2009	PM_{10}	μg/m³	D-A-33	20.5	21.1	-	–	–	✓	5.4
2009	PAH	μg/m³	D-A-32	98.7	68.6	Top	✓	–	✓	73.7
2009	PAH	μg/m³	W-A-3	149.8	68.6	Top	✓	✓	✓	–

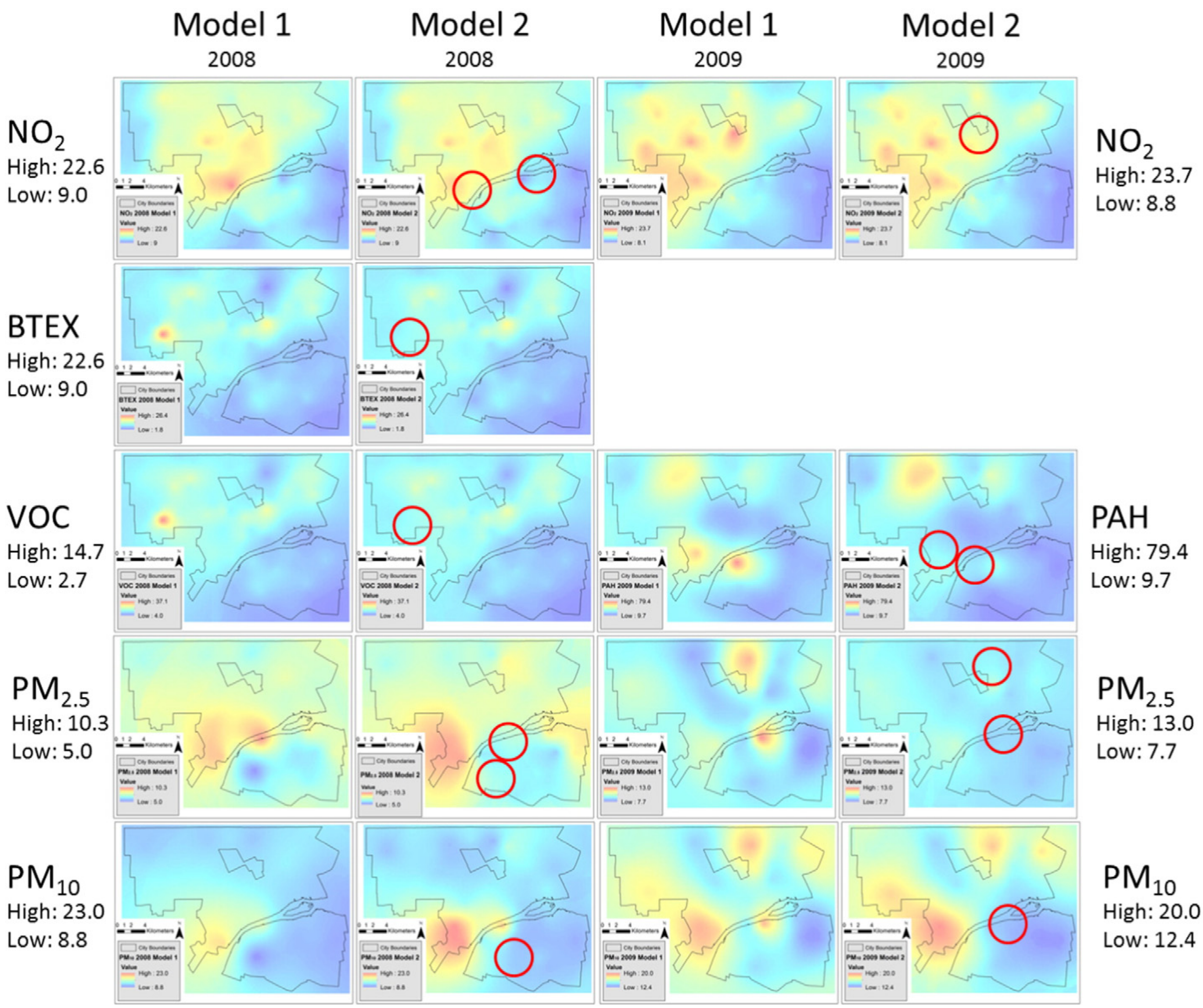

Fig. 8. Comparison Model 1 and Model 2 with former outlier locations circled.

additional potential outliers identified by two of four methods were also selected. These included global outliers evident on box plots that were also clearly identifiable as anomalies on the difference maps. Less obvious were four potential outliers that showed agreement between box plot and variogram cloud, but were not recognized using difference maps or Moran's I. These were ultimately excluded.

Among the final group of 13 outliers selected, one or more outliers were identified for each analyte in each year except for BTEX and VOCs, which lacked outliers in 2009, and PAH, which lacked outliers in 2008. Two outliers were identified for NO_2 and $PM_{2.5}$ in 2008 and for PAH and $PM_{2.5}$ in 2009 (Table 2).

3.3. Air pollution model revisions

Model 2 was created with revised variograms and ordinary kriged grids computed from the datasets with the outliers removed. Although both Models 1 and 2 interpolate over a larger area than the Detroit and Windsor municipal borders (Fig. 8), quantitative model comparisons were restricted to grid nodes located within Detroit (including Hamtramck and Highland Park) and Windsor city boundaries.

Model 2 employed different variogram and kriging parameters (Table 3) than Model 1. Model 2 sill contributions were lower for NO_2, BTEX, VOCs, and PAH. As a result, ranges and standard deviations of the interpolated distributions for NO_2, BTEX, and VOCs were reduced in Model 2 compared to Model 1 (Table 4). Conversely, standard deviations increased markedly for PM_{10} and slightly for $PM_{2.5}$ and PAHs in Model 2 compared to Model 1. Different versions of the PM datasets were used for Models 1 and 2 (Section 2.3), so direct comparisons between these models are not meaningful.

Table 3
Variogram model and kriging parameters for Model 2 with outliers removed.

Pollutant	Year	Model	Nugget	Relative nugget (%)	Sill contribution	Range (m)	Search radius (m)
NO_2	2008	Exponential	0.75	9	8	15,000	10,000
NO_2	2009	Spherical	1.3	11	11	16,000	10,000
BTEX	2008	Exponential	0.57	5	11	11,500	10,000
VOC	2008	Exponential	2.1	9	21	16,000	10,000
PAH	2009	Spherical	25	11	200	10,000	20,000
$PM_{2.5}$	2008	Spherical	0.2	13	1.35	7,000	20,000
$PM_{2.5}$	2009	Spherical	0.5	50	0.5	7,000	20,000
PM_{10}	2008	Spherical	0.03	<1	11.7	13,000	20,000
PM_{10}	2009	Spherical	1.5	25	4.5	10,000	20,000

Table 4
Comparison of kriged model statistics for Models 1 and 2.

Year	Analyte	Unit	Model #	Mean	Min	Max	Range	STD	% diff. of STD
2008	NO_2	ppb	Model 1	15.2	9.1	22.6	13.4	2.42	−4.2
2008	NO_2	ppb	Model 2	15.2	9.1	20.0	10.9	2.32	
2009	NO_2	ppb	Model 1	15.1	8.2	23.6	15.4	3.16	−4.9
2009	NO2	ppb	Model 2	14.9	8.1	22.6	14.4	3.01	
2008	BTEX	$\mu g/m^3$	Model 1	8.8	1.9	26.4	24.5	2.96	−14.4
2008	BTEX	$\mu g/m^3$	Model 2	8.7	1.9	18.1	16.2	2.56	
2008	VOC	$\mu g/m^3$	Model 1	13.7	4.1	37.0	33.0	4.12	−13.1
2008	VOC	$\mu g/m^3$	Model 2	13.5	4.1	23.5	19.4	3.61	
2008	$PM_{2.5}$	$\mu g/m^3$	Model 1	7.7	5.1	10.1	5.0	0.67	−9.9
2008	$PM_{2.5}$	$\mu g/m^3$	Model 2	7.8	6.0	10.0	4.0	0.74	
2009	$PM_{2.5}$	$\mu g/m^3$	Model 1	9.6	7.7	13.0	5.2	0.77	−73.1
2009	$PM_{2.5}$	$\mu g/m^3$	Model 2	9.2	8.3	10.3	2.0	0.36	
2008	PM_{10}	$\mu g/m^3$	Model 1	12.7	8.8	19.6	10.8	1.89	22.1
2008	PM_{10}	$\mu g/m^3$	Model 2	13.1	10.0	22.9	13.0	2.36	
2009	PM_{10}	$\mu g/m^3$	Model 1	15.9	12.6	19.2	6.6	1.31	21.3
2009	PM_{10}	$\mu g/m^3$	Model 2	15.6	12.5	19.9	7.4	1.62	
2009	PAH	$\mu g/m^3$	Model 1	31.8	13.3	79.3	66.1	11.0	4.3
2009	PAH	$\mu g/m^3$	Model 2	28.4	10.0	65.1	55.1	11.5	

Models 3 and 4 were created from Models 1 and 2, respectively, using temporal scaling for Detroit (Fig. 2). Model 4, with outliers removed, exhibits reduced variability compared to Model 3 with smaller ranges and standard deviations across Detroit for NO_2, BTEX, and $PM_{2.5}$ (Table 5). The range and standard deviation of PM_{10} values is greater for Model 3 versus Model 4, but differences in the construction of PM models confounds direct comparison.

In several cases, the removal of outliers changed grid interpolation values in areas up to 20 km from the outlier locations (Fig. 8). Although spatial changes were expected to occur in areas of close proximity to where outliers were removed, the degree of distance where grid nodes were affected was unanticipated. These changes are attributable to a combination of effects stemming from outlier removal including changes to variogram models and recalculation of kriging weights based on the revised distribution of control points. Because variograms exert a universal impact on ordinary kriged interpolation grids while outliers have a local impact based on the kriging search radius, observed model changes are more likely the result of variogram revisions after outlier removal.

3.4. Asthma associations

2008 asthma associations with air pollution Models 1 and 2 were compared for both Detroit (Table 6) and Windsor (Table 7). In Detroit, outlier removal decreased coefficient of determination (r^2) values for BTEX and VOCs. Model 2 asthma associations remained statistically significant (p-value ≤ 0.05) for BTEX but not VOCs (Table 6). Outlier removal increased r^2 values for NO_2, $PM_{2.5}$, and PM_{10} asthma associations in Detroit, although they remained statistically insignificant. In Windsor, asthma associations with NO_2, VOCs, and PM_{10} were statistically significant for Model 1 but only the association with NO_2 was significant for Model 2 (Table 7). With the exception of $PM_{2.5}$, which was not statistically significant, r^2 values decreased in Windsor indicating weaker correlations between asthma and air pollution with outliers removed.

2008 asthma associations with air pollution Models 3 and 4, which include temporal scaling, were evaluated for Detroit (Table 6). NO_2 and BTEX associations were statistically significant for Models 3 and 4. In general, the addition of temporal scaling increased the strength of asthma associations and the exclusion of outliers had mixed results. Temporal scaling (Model 3 vs. Model 1) improved r^2 and p-values for NO_2, BTEX, and $PM_{2.5}$. Removal of outliers in temporally scaled models (Model 4 vs. Model 3) improved asthma associations for NO_2 and PM_{10}, but decreased associations for BTEX and $PM_{2.5}$.

All but one of the statistically significant asthma associations identified (Tables 6 and 7) involved analytes measured with passive samplers (NO_2, VOCs, and BTEX) rather than analytes measured with active samplers (PM). This suggests greater sensitivity with higher spatial sample density and may indicate that a minimum sample spacing of approximately 1 per 5 km^2 is needed to adequately model neighborhood-scale spatial variability of the air pollutants using kriging as applied in this study. Alternatively, incorporation of secondary information on spatial variability may help to improve exposure classification, particularly when integrated with temporal pollutant measurements (e.g., Shmool et al., 2016).

Removing outliers decreased the range of modeled concentrations in Model 2 (Table 4) and Model 4 (Table 5). In most cases, outlier removal excluded extreme measurement values that influenced kriged model estimates in the vicinity of outlier locations, as well as average pollutant concentration estimates across the postal code areas that contain them. Thus, the decreased range may have had an adverse effect on the sensitivity of statistical relationships between air pollution and asthma exacerbations assessed using linear regression.

3.5. Limitations

Air pollution modeling in this study was informed by a high density spatial distribution of sample locations in the Detroit-Windsor urban airshed. Nevertheless, the effectiveness of the Local Moran's I test for outlier identification may have been limited by the spatial density of

Table 5
Comparison of temporally adjusted model statistics for Models 3 and 4.

Year	Analyte	Unit	Model #	Mean	Min	Max	Range	STD	% diff. of STD
2008	NO_2	ppb	Model 3	18.0	12.7	22.8	10.1	1.88	−10.1
2008	NO_2	ppb	Model 4	17.9	12.9	22.9	10.0	1.70	
2008	BTEX	$\mu g/m^3$	Model 3	8.4	3.9	18.8	15.0	1.70	−19.4
2008	BTEX	$\mu g/m^3$	Model 4	8.3	3.9	14.7	10.9	1.40	
2008	$PM_{2.5}$	$\mu g/m^3$	Model 3	11.2	10.0	12.3	2.3	0.45	−19.5
2008	$PM_{2.5}$	$\mu g/m^3$	Model 4	11.0	10.3	12.3	1.6	0.37	
2008	PM_{10}	$\mu g/m^3$	Model 3	16.6	14.5	21.0	6.5	1.31	27.1
2008	PM_{10}	$\mu g/m^3$	Model 4	16.2	13.8	22.8	9.0	1.72	

Table 6
Asthma associations for Detroit. Model 1 values from Lemke et al. (2014). Statistically significant associations are bold. Models 3 and 4 did not include VOCs.

GeoDHOC Detroit				
Year	Analyte	Model #	r^2	p-Value
2008	NO_2	Model 1	0.03	0.40
2008	NO_2	Model 2	0.04	0.32
2008	**NO_2**	**Model 3**	**0.16**	**0.05**
2008	**NO_2**	**Model 4**	**0.19**	**0.03**
2008	**BTEX**	**Model 1**	**0.28**	**0.01**
2008	**BTEX**	**Model 2**	**0.18**	**0.03**
2008	**BTEX**	**Model 3**	**0.32**	**<0.01**
2008	**BTEX**	**Model 4**	**0.26**	**0.01**
2008	**VOC**	**Model 1**	**0.26**	**0.01**
2008	VOC	Model 2	0.14	0.07
2008	$PM_{2.5}$	Model 1	<0.01	0.84
2008	$PM_{2.5}$	Model 2	<0.01	0.80
2008	$PM_{2.5}$	Model 3	0.05	0.29
2008	$PM_{2.5}$	Model 4	0.02	0.52
2008	PM_{10}	Model 1	<0.01	>0.99
2008	PM_{10}	Model 2	0.06	0.24
2008	PM_{10}	Model 3	<0.01	0.79
2008	PM_{10}	Model 4	0.04	0.36

available air pollution measurements, particularly for analytes measured with fewer active monitors deployed at greater spacing. Temporal resolution of the spatially distributed measurements was limited to two, two-week sampling periods spaced nine months apart, although measurements were augmented by time series data recorded at MASN community air quality monitoring stations in Detroit.

Asthma associations in this study were limited by the assignment of air pollution exposure estimates based on modeled ambient air concentrations rather than personal exposure which can lead to potential error (Koehler and Peters, 2015). Moreover, the asthma events were reported by postal code which decreased the effective spatial resolution of the air pollutant models from a 300 by 300 meter grid spacing to aggregate zip code or forward sortation area scale averages. In addition, the asthma data were aggregated on a yearly basis and did not account for temporal variation throughout the year. Finally, the results of the correlation do not account for differences in socioeconomic demographics or medical management of asthma (Lemke et al., 2014). Nevertheless, results demonstrate that the identification and exclusion of outliers from urban air pollution datasets influences both ambient air pollution models and their association with health outcomes aggregated at a postal code scale.

4. Conclusions

A multi-step approach was employed to identify spatio-temporal outliers in Detroit and Windsor air pollutant concentration measurements collected in September 2008 and June 2009. Unlike previous studies which relied upon a single method to identify outliers (e.g., Miller, 2012) or did not explicitly assess effects of outlier removal (e.g., Clougherty et al., 2013), this study employed multiple methods to identify outliers and evaluated the consequences of their removal on a health outcome.

Four alternative outlier identification methods were evaluated. Box plots, variogram clouds, and difference maps determined the final set of outliers. The Moran's I statistic was not useful for outlier identification in the datasets studied. Conformity of results among box plots, variogram clouds, and difference maps when applied in combination strengthened the analysis of outlier identification and influence. It is therefore recommended that two or more approaches, including both local and global methods, be employed jointly for outlier identification in urban air quality datasets.

Outlier removal changed local values and, in some instances, the spatial distribution of concentrations in revised ordinary kriged air pollution models. These changes are attributable to the absence of individual control points as well as the subsequent adjustment of variogram models. Thus, outlier removal produced changes in the vicinity of measurement points that were removed, and influenced global air pollution model statistics.

Overall, associations between air pollution and asthma hospitalizations were weakened with outlier removal but improved with the addition of temporal data. With outliers removed, modeled pollutant concentration ranges (the independent variable used for linear regression) became smaller, and there were fewer statistically significant associations between air pollutants and asthma. Incorporating temporal scaling to reflect trends recorded by MASN time series measurements increased the number of statistically significant pollutant-asthma associations.

Although the models generated by this study provide a detailed set of alternative air pollution models in Detroit and Windsor, future studies should reassess associations with asthma and other relevant health outcomes using better resolved spatial and temporal information to reduce potential exposure misclassification. Refining the spatial resolution of asthma events to the neighborhood level using residential addresses and increasing the temporal resolution of asthma data to monthly counts, commensurate with the air pollution model temporal resolution, could improve asthma-pollutant associations.

Table 7
Asthma associations for Windsor. Model 1 values from Lemke et al. (2014). Statistically significant associations are bold.

GeoDHOC Windsor				
Year	Analyte	Model #	r^2	p-Value
2008	**NO_2**	**Model 1**	**0.39**	**0.03**
2008	**NO_2**	**Model 2**	**0.35**	**0.04**
2008	BTEX	Model 1	0.18	0.16
2008	BTEX	Model 2	0.13	0.24
2008	**VOC**	**Model 1**	**0.34**	**0.05**
2008	VOC	Model 2	0.25	0.10
2008	$PM_{2.5}$	Model 1	0.10	0.33
2008	$PM_{2.5}$	Model 2	0.16	0.21
2008	**PM_{10}**	**Model 1**	**0.37**	**0.04**
2008	PM_{10}	Model 2	0.23	0.11

Acknowledgements

Funding for this project was provided by a grant from the W.K. Kellogg Foundation, P3018205, and through a Wayne State University Career Development Grant. MASN data were provided by the Michigan Department of Environmental Quality (MDEQ) Air Quality Division. The authors thank Gianluca Sperone at Wayne State University for technical support and acknowledge valuable technical discussions with Craig Fitzner, Debbie Sherrod, and Amy Robinson at the MDEQ. The content of this article is solely the responsibility of its authors.

Appendix A. Supplementary data

Supplementary data to this article can be found online at http://dx.doi.org/10.1016/j.scitotenv.2016.08.031.

References

Anastasopoulos, A.T., Wheeler, A.J., Karman, D., Kulka, R.H., 2012. Intraurban concentrations, spatial variability and correlation of ambient polycyclic aromatic hydrocarbons (PAH) and PM2.5. Atmos. Environ. 59, 272–283. http://dx.doi.org/10.1016/j.atmosenv.2012.05.004.
Anselin, L., 1995. Local Indicators of Spatial Association—LISA. Geogr. Anal. 27 (2), 93–115. http://dx.doi.org/10.1111/j.1538-4632.1995.tb00338.x.
Barnett, V., Lewis, T., 1994. Outliers in Statistical Data. New York, John Wiley, New York (584 p).

Clougherty, J.E., Kheirbek, I., Eisl, H.M., Ross, Z., Pezeshki, G., Gorczynski, J.E., Johnson, S., Markowitz, S., Kass, D., Matte, T., 2013. Intra-urban spatial variability in wintertime street-level concentrations of multiple combustion-related air pollutants: the New York City Community Air Survey (NYCCAS). Journal of Exposure Science and Environmental Epidemiology 23 (3), 232–240. http://dx.doi.org/10.1038/jes.2012.125.

Dai, X., Jin, L., Shi, A., Shi, L., 2016. Outlier detection and accommodation in general spatial models. Statistical Methods & Applications 1–23. http://dx.doi.org/10.1007/s10260-015-0348-1.

Ernst, M., Haesbroeck, G., 2016. Comparison of Local Outliers Detection Techniques in Spatial Multivariate Data. http://dx.doi.org/10.1007/s10618-016-0471-0.

Fu, W., Zhao, K., Zhang, C., Wu, J., Tunney, H., 2016. Outlier identification of soil phosphorus and its implication for spatial structure modeling. Precis. Agric. 17 (2), 121–135. http://dx.doi.org/10.1007/s11119-015-9411-z.

Haslett, J., Bradley, R., Craig, P., Unwin, A., Wills, G., 1991. Dynamic graphics for exploring spatial data with application to locating global and local anomalies. Am. Stat. 45 (3), 234–242. http://dx.doi.org/10.2307/2684298.

Isaaks, E.H., Srivastava, R.M., 1989. An Introduction to Applied Geostatistics. Oxford University Press, New York, New York (561 p).

Kiefer, N.M., Salmon, M., 1983. Testing normality in econometric models. Econ. Lett. 11 (1–2), 123–127.

Koehler, K.A., Peters, T.M., 2015. New methods for personal exposure monitoring for airborne particles. Current Environmental Health Reports 2 (4), 399–411. http://dx.doi.org/10.1007/s40572-015-0070-z.

Kracht, O., Reuter, H.I., Gerboles, M., 2013. A spatio-temporal screening tool for outlier detection in long term/large scale air quality observation time series and monitoring networks [abs.]. EGU General Assembly 2013, Vienna, Austria, 7–12 April of Conference.

Lemke, L.D., Lamerato, L.E., Xu, X., Booza, J.C., Reiners, J.J., Raymond Iii, D.M., Villeneuve, P.J., Lavigne, E., Larkin, D., Krouse, H.J., 2014. Geospatial relationships of air pollution and acute asthma events across the Detroit-Windsor international border: study design and preliminary results. J. Expos. Sci. Environ. Epidemiol. 24 (4), 346–357. http://dx.doi.org/10.1038/jes.2013.78.

Li, L., Wu, J., Ghosh, J.K., Ritz, B., 2013. Estimating spatiotemporal variability of ambient air pollutant concentrations with a hierarchical model. Atmos. Environ. 71, 54–63. http://dx.doi.org/10.1016/j.atmosenv.2013.01.038.

Li, W., Xu, B., Song, Q., Liu, X., Xu, J., Brookes, P.C., 2014. The identification of 'hotspots' of heavy metal pollution in soil–rice systems at a regional scale in eastern China. Sci. Total Environ. 472, 407–420. http://dx.doi.org/10.1016/j.scitotenv.2013.11.046.

MDEQ, 2008. 2008 Annual Air Quality Report. http://www.michigan.gov/documents/deq/deq-aqd-air-2008-Air-Quality-Report_296426_7.pdf.

MDEQ, 2013. Michigan's 2014 Ambient Air Monitoring Network Review. http://www.michigan.gov/documents/deq/deq-aqd-aqe-monitoring-network-review-2014_426389_7.pdf.

Miller, L., 2012. A Long Term Geospatial Investigation of Air Quality in Windsor, Ontario, Canada - Comparison to Nearby Cities and Applications of Inter-species Ratios (NR78853 Ph.D.) University of Windsor, Canada (239 p).

Miller, L., Lemke, L.D., Xu, X., Molaroni, S.M., You, H., Wheeler, A.J., Booza, J., Grgicak-Mannion, A., Krajenta, R., Graniero, P., 2010. Intra-urban correlation and spatial variability of air toxics across an international airshed in Detroit, Michigan (USA) and Windsor, Ontario (Canada). Atmos. Environ. 44 (9), 1162–1174. http://dx.doi.org/10.1016/j.atmosenv.2009.12.030.

O'Leary, B.F., 2014. Evaluating Spatial Outliers and Integrating Temporal Data in Air Pollution Models for the Detroit-Windsor Airshed M.S. Thesis Wayne State University, Detroit, Michigan 9781321183092, p. 168.

O'Leary, B.F., Lemke, L.D., 2014. Modeling spatiotemporal variability of intra-urban air pollutants in Detroit: a pragmatic approach. Atmos. Environ. 94, 417–427. http://dx.doi.org/10.1016/j.atmosenv.2014.05.010.

Schubert, E., Zimek, A., Kriegel, H.-P., 2014. Local outlier detection reconsidered: a generalized view on locality with applications to spatial, video, and network outlier detection. Data Min. Knowl. Disc. 28 (1), 190–237. http://dx.doi.org/10.1007/s10618-012-0300-z.

Sguera, C., Galeano, P., Lillo, R.E., 2016. Functional outlier detection by a local depth with application to NO x levels. Stoch. Env. Res. Risk A. 30 (4), 1115–1130. http://dx.doi.org/10.1007/s00477-015-1096-3.

Shmool, J.L.C., Kinnee, E., Sheffield, P.E., Clougherty, J.E., 2016. Spatio-temporal ozone variation in a case-crossover analysis of childhood asthma hospital visits in New York City. Environ. Res. 147, 108–114. http://dx.doi.org/10.1016/j.envres.2016.01.020.

Szpiro, A.A., Sampson, P.D., Sheppard, L., Lumley, T., Adar, S.D., Kaufman, J., 2009. Predicting intra-urban variation in air pollution concentrations with complex spatio-temporal dependencies. Environmetrics 21 (6), 606–631. http://dx.doi.org/10.1002/env.1014.

Walker, I.J., Eamer, J.B.R., Darke, I.B., 2013. Assessing significant geomorphic changes and effectiveness of dynamic restoration in a coastal dune ecosystem. Geomorphology 199, 192–204. http://dx.doi.org/10.1016/j.geomorph.2013.04.023.

Wu, J., Edwards, R., He, X., Liu, Z., Kleinman, M., 2010. Spatial analysis of bioavailable soil lead concentrations in Los Angeles, California. Environ. Res. 110 (4), 309–317. http://dx.doi.org/10.1016/j.envres.2010.02.004.

Zhang, C., McGrath, D., 2004. Geostatistical and GIS analyses on soil organic carbon concentrations in grassland of southeastern Ireland from two different periods. Geoderma 119 (3–4), 261–275. http://dx.doi.org/10.1016/j.geoderma.2003.08.004.

Zhang, C., Luo, L., Xu, W., Ledwith, V., 2008. Use of local Moran's I and GIS to identify pollution hotspots of Pb in urban soils of Galway, Ireland. Sci. Total Environ. 398 (1–3), 212–221. http://dx.doi.org/10.1016/j.scitotenv.2008.03.011.

Zou, B., Peng, F., Wan, N., Mamady, K., Wilson, G.J., 2014. Spatial cluster detection of air pollution exposure inequities across the United States. PLoS ONE 9 (3), e91917. http://dx.doi.org/10.1371/journal.pone.0091917.